

# High Precision Fault-Tolerant Quantum Circuit Synthesis by Diagonalization using Reinforcement Learning

MATHIAS WEIDEN, The University of California, Berkeley, USA

JUSTIN KALLOOR, The University of California, Berkeley, USA

ED YOUNIS, Lawrence Berkeley National Laboratory, USA

JOHN KUBIATOWICZ, The University of California, Berkeley, USA

COSTIN IANCU, Lawrence Berkeley National Laboratory, USA

Resource efficient and high precision compilation of programs into quantum circuits expressed in Fault-Tolerant gate sets, such as the Clifford+T gate set, is vital for the success of quantum computing. Optimal analytical compilation methods are known for restricted classes of unitaries, otherwise the problem is intractable. Empirical search-based synthesis methods, including Reinforcement Learning and simulated annealing, can generate good implementations for a more extensive set of unitaries, but require trade-offs in approximation precision and resource use. We leverage search-based methods to reduce the general unitary synthesis problem to one of synthesizing diagonal unitaries; a problem solvable efficiently in general and optimally in the single-qubit case. We demonstrate how our approach improves the implementation precision attainable by Fault-Tolerant synthesis algorithms on an array of unitaries taken from real quantum algorithms. On these benchmarks, many of which cannot be handled by existing approaches, we observe an average of 95% fewer resource-intensive non-Clifford gates compared to the more general Quantum Shannon Decomposition. On a subset of algorithms of interest for future term applications, diagonalization can reduce T gate counts by up to 16.8% compared to other methods.

CCS Concepts: • **Hardware** → **Quantum error correction and fault tolerance**; • **Computing methodologies** → *Reinforcement learning*; • **Software and its engineering** → *Compilers*.

Additional Key Words and Phrases: Quantum Compilation, Reinforcement Learning, Unitary Synthesis, Fault Tolerance

## 1 Introduction

Recent small scale demonstrations of logical qubits [5, 13] signal significant progress towards the development of Fault-Tolerant (FT) quantum computers. In this regime, a quantum program must be translated, or transpiled, into a quantum circuit (sequence of instructions) which uses only operations from a FT gate set. These discrete sets of gates consist of Clifford gates (e.g. H, S, CNOT) augmented with at least one non-Clifford gate (e.g. T or V) for universality. The Clifford+T gate set is one such universal FT gate set and is the target of many FT quantum compilation algorithms [16, 23–25, 48]. As executing non-Clifford gates in many models of FT computation requires expensive pre-processing in the form of magic state distillation [8, 29], a common goal of code generation tools is minimizing the number of non-Clifford gates used while transpiling some target program.

The function of any  $n$ -qubit quantum circuit is fully specified by a unitary matrix  $U \in \mathbb{U}(2^n)$ . As illustrated in Figure 1, existing FT compilation algorithms must trade-off between the quality of the solution (e.g. T gate count or depth), implementation precision (i.e. approximation error) and generality (i.e. unitary domain). The approximation error of a circuit measures the closeness of an algorithm’s implementation to the intended target program. Although the

---

Authors’ Contact Information: Mathias Weiden, mtweiden@berkeley.edu, The University of California, Berkeley, Berkeley, California, USA; Justin Kalloor, jkalloor3@berkeley.edu, The University of California, Berkeley, Berkeley, California, USA; Ed Younis, edyounis@lbl.gov, Lawrence Berkeley National Laboratory, Berkeley, California, USA; John Kubiatowicz, kubitron@cs.berkeley.edu, The University of California, Berkeley, Berkeley, California, USA; Costin Iancu, cciancu@lbl.gov, Lawrence Berkeley National Laboratory, Berkeley, California, USA.

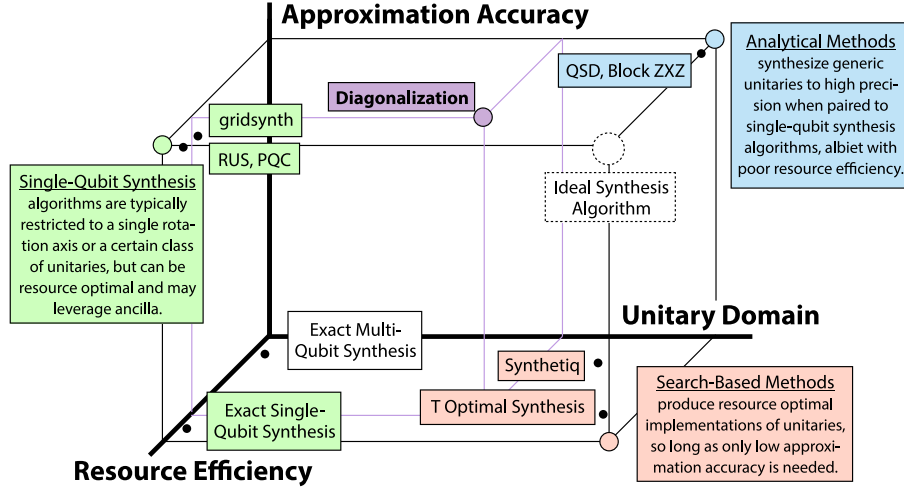


Fig. 1. Tradeoffs for synthesis algorithms targeting the Clifford+T gate set. *Approximation accuracy* refers to the precision with which a target program is implemented. In the FT setting, this value must be high in order for program outputs to be meaningful. *Resource efficiency* refers to non-Clifford gate counts. As these gates are orders of magnitude more expensive than Clifford gates, synthesis algorithms should use as few non-Clifford gates as possible. *Unitary domain* refers to how general the class of unitaries that can be taken as input is. This ranges from exactly synthesizable unitaries and approximations of 1-qubit  $R_Z$  rotations, to the most general class of all multi-qubit unitaries.

specific level of approximation error required for high-fidelity representation depends on the algorithm, low-precision synthesis eliminates the ability of synthesis algorithms to act as transpilers for future-term algorithms (see Section 6).

If every element of a unitary is in the ring  $\mathbb{Z}[e^{i\pi/4}, \frac{1}{2}]$ , it can be implemented exactly with the Clifford+T gate set [21, 28]. Unitaries which appear in real algorithms are rarely this well structured, meaning approximation is necessary. Luckily, the universal Clifford+T gate set can approximate any unitary transformation [27]. General analytical decomposition methods [15, 44] paired with single-qubit Clifford+T synthesis algorithms can handle any unitary, but the resultant circuits often contain an exponential ( $O(4^N)$ ) number of gates. In restricted cases (i.e. single qubit  $R_Z$  rotations), optimal approximate Clifford+T implementations of unitaries can be efficiently found [43]. Beyond single-qubit rotations restricted to a single axis, finding optimal approximate implementations of unitaries in the Clifford+T gate set is intractable [22].

*Search-based* circuit synthesis methods perform discrete searches through the space of possible quantum gate placements [2, 20, 37]. Search-based algorithms can discover more efficient circuits than analytical methods, but fail when low approximation error is needed. Because continuously parameterized unitary rotation operations typically correspond to very long sequences of discrete gates (see Figure 2), existing methods fail to converge when compiling high precision implementations of complex unitaries.

Thus, the state-of-the-art in compiling FT circuits can be summarized as follows: we can generate precise implementations of arbitrary unitaries using a large number of resources, and we can generate resource efficient but highly coarse approximations of unitaries. Our work advances search-based FT circuit compilation in both precision and generality:

(1) We improve the approximation precision of multi-qubit synthesis algorithms on unitaries taken from real benchmarks. The main idea is to diagonalize rather than invert unitaries during synthesis. This allows us to bypass the

need to transpose difficult single-qubit rotations with search-based tools. Instead we use optimal analytical techniques to implement complex single-qubit rotations. Diagonalization produces high precision results when state-of-the-art search-based tools fail. This approach is general; other search-based tools can be retrofitted for diagonalization.

(2) Our Diagonalizing Value Network for Unitaries (DVNU) approach advances the state-of-the-art for RL-based synthesis methods by broadening the scope of circuits which can be synthesized using deep learning. We introduce two novel ideas: i) a global-phase invariance operation which alleviates the requirement that networks themselves learn invariant representations; ii) unitary perturbations applied during learning which force neural networks to associate a learned value with a region instead of a point. These methods can be applied to any existing machine-learning-based workflow that targets datasets which consist of unitary matrices.

Our data indicate that the relaxation to diagonalization along with our neural architectural changes enable efficient and high precision synthesis of unitaries from real quantum algorithms. Our RL-based approach leads to fast inference and it is practical for use as a component in a full stack quantum compiler. When compared with existing techniques, we improve precision by several orders of magnitude. By parameterizing continuous rotations, diagonalization enables for techniques such unitary mixing to boost precision even further [10]. Synthesis using diagonalization also reduces T gate counts by up to 16.8% compared to existing techniques.

The remainder of the paper is organized as follows: Section 2 discusses necessary background information relating to synthesis with discrete gate sets. Section 3 explains how matrix diagonalization can be framed in the language of synthesis. Section 4 introduces neural network architectural developments natural for quantum datasets. Section 5 evaluates the new architecture on synthesis tasks and shows how our RL-based approach can effectively synthesize many unitaries taken from partitioned quantum algorithms. Section 6 discusses methods of scaling, interprets the learned value function, and argues for the utility of RL in unitary synthesis. Finally, Section 7 offers concluding remarks.

## 2 Background

Universal quantum computers must implement complex unitaries (programs) with high fidelity. Noisy Intermediate Scale Quantum (NISQ) gate sets typically consist of an entangling two-qubit gate (e.g. CNOT or CZ gates) along with a set of fixed and continuously parameterized single-qubit gates (e.g.  $X$  and  $R_Z(\theta)$ ).

FT quantum computing differs in that it relies on quantum error correction, which restricts the kinds of operations that can be used. Quantum error correcting codes encode the state of one or more *logical* qubits into many *physical* qubits [45]. Some logical operations require only that the same physical operation be applied to each physical qubit. These *transversal* gates form closed finite groups and are not universal [17]. The Clifford group coincides with the transversal gate set of many codes of interest. For universal quantum computation, the logical gate set must contain a non-transversal operation. This additional non-transversal gate is typically assumed to be the T gate, as such this work will focus on the approximate compilation of unitaries into the Clifford+T gate set. However, this method is extensible to a number of other "magic" gates.

The T gate can be executed in a fault-tolerant manner through magic state distillation and injection with Clifford gate corrections [35]. However, state distillation is extremely costly. Estimates show that up to 99% of the resources on a quantum computer could be dedicated to the implementation of these operations [19, 36]. Minimizing the number of T gates for a given implementation of a unitary is therefore an essential step in the realization of practical error corrected quantum computation.

## 2.1 Fault-Tolerant Unitary Synthesis

A quantum program can be described as a circuit, or sequence of quantum gates. A unitary (or quantum circuit) synthesis algorithm prepares a circuit which implements some target unitary matrix. This implementation can be exact (e.g. zero error or zero process distance) or approximate. Exact synthesis is only possible for a very restricted subset of programs (unitaries). Only if every element of a unitary is in the ring  $\mathbb{Z}[e^{i\pi/4}, \frac{1}{2}]$  can it be implemented exactly with the Clifford+T gate set [21, 28]. Unitaries which appear in real algorithms are rarely this well structured, meaning approximation is necessary.

Say that we want to synthesize the unitary labeled *Target* in Figure 2. In the most general solution, as a first step, the unitary is decomposed using non-FT gates so that the program is expressed as a sequence of CNOT and general single-qubit unitary gates (any  $2 \times 2$  unitary matrix). The Quantum Shannon Decomposition and its variants are able to produce circuit implementations which approach the asymptotic lower bound of  $O(4^n)$  CNOT and  $R_Z$  gates [15, 44]. Other numerical-optimization-based synthesis approaches can generate far more efficient circuits at the expense of compilation time [14, 49]. Although these approaches can always be applied and allow for low approximation error, they still often produce circuits which contain many non-Clifford gates.

The second compilation step entails translating non-Clifford gates into a FT gate set. The most generic approach decomposes single-qubit unitaries into  $\sqrt{X}$  (Clifford) and  $R_Z(\theta)$  (non-Clifford) gates. For some precision  $\epsilon$ , translating  $R_Z$  operations into Clifford+T gates requires  $O(\log \frac{1}{\epsilon})$  gates. Except in select cases (i.e.  $\theta \in \{\frac{k\pi}{4} : k \in \mathbb{Z}\}$ ) this is true regardless of the angle of rotation.  $R_Z$  rotations can be approximated *optimally* in the ancilla-free case to arbitrary precision using the *gridsynth* algorithm [43]. As a frame of reference, synthesizing a single  $R_Z$  gate to a precision of  $\epsilon \leq 10^{-8}$  requires  $\approx 200$  Clifford+T gates. Ancilla-based methods can generate more resource efficient circuits than *gridsynth* [6, 7, 30], and advances in unitary synthesis algorithms promise to discover more such methods.

Another option is to deploy a synthesis algorithm which uses a guiding function to iteratively modify a circuit, often gate-by-gate, until the target unitary is implemented. These *search-based* approaches generate more resource efficient circuits than the previously described generic analytical workflow. Examples of such algorithms include Reinforcement

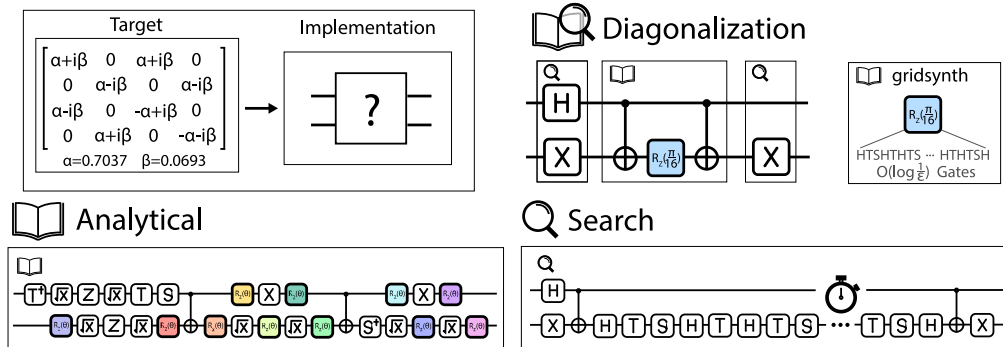


Fig. 2. Comparison of analytical, search-based, and diagonalization strategies for Clifford+T synthesis. Analytical decomposition approaches, such as the Quantum Shannon Decomposition, are universally applicable but often produce poor quality results. Search-based methods are able to find very high quality (low gate count) approximations, but are intractable except at low precision and low qubit count. Diagonalization is a hybrid approach that enables both high quality and high precision. *gridsynth* [43] is used to optimally decompose continuous single-qubit  $R_Z$  operations (colored boxes) into Clifford+T gates.

Learning approaches [1, 11, 34, 41, 57], simulated annealing [37], and several optimal and heuristic synthesis algorithms [2, 20, 22]. Empirically, these state-of-the-art methods are able to find very efficient implementations of multi-qubit unitaries so long as solutions require few (meaning on the order of tens of) gates. Search-based tools are restricted in that they only operate with discrete gate sets, thus they have no direct way of handling continuous rotations such as  $R_Z$  gates. For unitaries which contain these rotations, which are ubiquitous in unitaries taken from real benchmarks of interest, search-based tools are only able to find low precision implementations for a subset of inputs.

## 2.2 Formalizing Unitary Synthesis

Unitary synthesis is typically framed as finding a circuit which inverts the adjoint (conjugate transpose) of the target matrix. When solving the problem directly by matrix inversion, every  $n$ -qubit circuit can be described as a sequence of primitive gates taken from a finite set  $A \subset \mathbb{U}(2^n)$ . Every primitive gate has a known associated unitary  $a \in A$ . Note that a gate’s unitary representation  $a$  depends both on the gate’s function and the qubit it acts on [35]. A circuit consisting of  $t$  gates can therefore be associated with a unitary matrix

$$C_t = a_t \times \dots \times a_1. \quad (1)$$

A quantum circuit with associated unitary  $C_t \in \mathbb{U}(2^n)$  is said to implement a target unitary matrix  $U_{tar} \in \mathbb{U}(2^n)$  when the distance condition

$$d_{HS}(C_t, U_{tar}) = \sqrt{1 - \frac{1}{4^n} |\text{Tr}(C_t U_{tar}^\dagger)|^2} \leq \epsilon \quad (2)$$

is satisfied. Here  $\epsilon \ll 1$  is a hyperparameter which determines how precisely a target must be implemented.

Synthesis methods that invert the adjoint of a target unitary using an FT gate set must find a (potentially very long) sequence of discrete gates which satisfies Equation 2. We propose an alternative approach: diagonalization (Figure 2). The diagonalization process consists of a two-headed search which halts when the target’s adjoint is diagonalized (i.e. not fully inverted). Diagonalizing ensures that up to  $2^n - 1$  continuous  $R_Z$  operations can be handled. Although there is no guarantee of optimality, this approach is able to find high precision implementations of complex unitaries (unlike search-based inversion methods), and produces significantly higher quality outputs than pure analytical methods (see Table 2). In the worst case, diagonalization acts exactly like the underlying search-based algorithm which implements it. When both diagonalization and search-based methods fail, analytical rule-based methods may be necessary.

Table 1 compares various unitary synthesis approaches which can be used to target the Clifford+T gate set. Among search-based methods, the simulated annealing tool *SynthetiQ* empirically finds better implementations of unitaries than other methods [37]. Even so, *SynthetiQ* fails to produce solutions for high precision implementations of complex unitaries as the space of circuits is too large to search. Synthesizing complex unitaries to high precision requires a mechanism for handling continuous rotations; this is possible in both analytical and diagonalization approaches.

## 2.3 Synthesis as a Markov Decision Process

Markov Decision Processes (MDPs) provide a framework for describing stochastic decision problems. Posing quantum circuit synthesis as an MDP has been demonstrated numerous times [1, 11, 34, 41, 57]. We define the MDP as a tuple  $(S, S_I, S_T, A, r, p)$ . Here  $S$  is a set of states,  $S_I$  a set of initial states,  $S_T$  a set of terminal states,  $A$  a set of actions or gates,  $r : S \times A \rightarrow \mathbb{R}$  a reward function, and  $p$  a distribution which assigns a probability to next states given a state-action pair. We use the term state (or sometimes unitary state) to describe an RL state  $s_t$ , not a quantum mechanical state vector or density operator.

Method	Qubits	Category	Precision	Unitary Domain
<i>gridsynth</i> [43]	1	Analytical	-	Approx. $R_Z$
Policy Iter. [1]	1	Search (RL)	$10^{-2}$	Approx. $\mathbb{U}(2)$
DQN [11]	1-2	Search (RL)	$10^{-3}$	Approx. $\mathbb{U}(2)$ - $\mathbb{U}(4)$
<i>SynthetiQ</i> [37]	1-4	Search (SA)	$10^{-3}$	Approx. $\mathbb{U}(2)$ - $\mathbb{U}(16)$
<b>DVNU</b> (ours)	1-3	Search (RL)	$10^{-6}$ and below	Approx. $\cup$ Diagonalizable $\mathbb{U}(2)$ - $\mathbb{U}(8)$
QSD [44]	1+	Analytical	-	$U \in \mathbb{U}(2^n)$

Table 1. Unitary synthesis approaches for the Clifford+T gate set. Among RL approaches, our Diagonalizing Value Network for Unitaries (DVNU) handles more complex inputs and with diagonalization can synthesize targets to very high precision. In cases where unitaries can be exactly diagonalized, DVNU can produce circuit implementations up to arbitrarily high precision. Precision here is measured using Hilbert-Schmidt distance (Eq 2). The *Unitary Domain* column indicates what kinds of unitaries can be handled. *SynthetiQ* uses simulated annealing and empirically outperforms other pure search-based tools at low precision. *gridsynth* optimally decomposes 1-qubit  $R_Z$  unitaries to any precision. The QSD is an analytical method which can be used along with *gridsynth* to synthesize Clifford+T circuits.

Given an MDP, a Reinforcement Learning (RL) algorithm optimizes for a policy which maximizes the total expected cumulative rewards. Formally, a policy denoted as  $\pi(a_t|s_t)$  assigns a probability to each possible action  $a_t \in A$  given state  $s_t$ . A state  $s_t$  has value

$$V^\pi(s_t) = \mathbb{E}_\pi \sum_{k=0}^T \gamma^k r(s_{t+k}, a_{t+k}) \quad (3)$$

where  $\gamma \in (0, 1]$  is a discount factor. The value is the expected cumulative discounted reward if policy  $\pi$  is followed. We can additionally define the state action value or *Q function*

$$Q^\pi(s_t, a_t) = r(s_t, a_t) + \gamma \mathbb{E}_p V^\pi(s_{t+1}) \quad (4)$$

which is the value of taking action  $a_t$  when in state  $s_t$  and then following policy  $\pi$ . Value functions differ from Q functions in that they only require a state, not a state-action pair.

RL algorithms typically consist of two entities, an *agent* and an *environment* (illustrated in Figure 3). The agent is trained in order to maximize the cumulative rewards it receives from the environment. Learning the optimal value function leads to a synthesis policy which produces circuit implementations of unitaries that contain the fewest possible gates. For the scope of this paper, a neural network is used to learn either a value function or a Q function. A policy can be obtained by simply taking the action which maximizes either function.

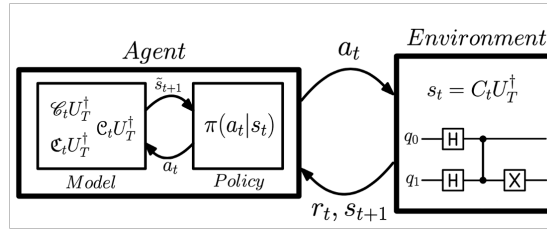


Fig. 3. A model-based Reinforcement Learning agent. The agent observes the state of the environment  $s_t$ , uses the policy to commit to an action  $a_t$ , then receives a reward  $r_t$ . Model-based synthesis approaches can evaluate the value of many actions before committing to them.

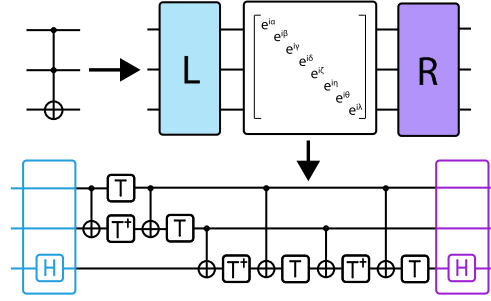


Fig. 4. Diagonalization ansatz for three-qubit unitaries. The diagonal matrix corresponds to  $2^n - 1$  continuous degrees of freedom which can be efficiently implemented with  $R_Z(\theta)$  and CNOT gates. The  $L$  and  $R$  subcircuits are made of discrete Clifford+T operations. A Toffoli only requires two H gates to be diagonalized and its diagonalization can be implemented with only CNOT and  $R_Z(\pm\frac{\pi}{4})$  ( $T$  or  $T^\dagger$  gates).

### 3 Diagonalization

Directly synthesizing a unitary by finding a sequence of gates which inverts it is intractable when high-precision is needed. This is because a large number of discrete gates are required to implement any single continuous rotation. To address this we shift the problem scope from inversion to diagonalization. This approach assumes there are continuous degrees of freedom in unitaries which cannot be handled by a search-based synthesis process. To fit the paradigm of search-based synthesis as described in Section 2.2, we first define the problem of diagonalization as an MDP. At time  $t \in \{0, 1, \dots, T\}$  in the synthesis process, the state  $s_t \in S$  is defined by

$$s_t = L_t U_{tar}^\dagger R_t \quad (5)$$

where  $L_t, R_t$  are each sequences of discrete operations (as in Equation 1). The set of initial states contains the adjoint of target unitaries  $S_I = \{U_{tar}^\dagger\}$ , meaning  $R_0 = L_0 = I_{2^n}$ . The set of terminal states is the set of all states which can be approximately inverted by a diagonal unitary matrix. This corresponds to the set of states satisfying

$$d_D(s_t) = \min_{\theta \in \mathbb{R}^{2^n}} d_{HS}(s_t, \exp(-i\theta \cdot \hat{\sigma})) \leq \epsilon \quad (6)$$

where  $\hat{\sigma}$  is the vector of all  $n$ -fold tensor products of the Pauli  $\sigma_I$  and  $\sigma_Z$  matrices. For brevity's sake, we denote the diagonal operator resulting from the matrix exponential as  $D_\theta$ . The reward function is an indicator function defined as

$$r(s_t) = \begin{cases} +1 & \text{if } s_t \in S_T \\ -1 & \text{else} \end{cases} \quad (7)$$

Given a terminal state  $s_T$ , the corresponding circuit is

$$R_T s_T^\dagger L_T = R_T D_\theta^{-1} L_T. \quad (8)$$

Figure 4 illustrates the general form of three-qubit circuits which satisfy this structure. As an example, the Toffoli gate can be diagonalized by just two Hadamard gates.

This process can be thought of as a Singular Value Decomposition where the left and right singular vector matrices are restricted to unitaries which can be efficiently implemented by searching through gate sequences from a discrete

gate set (i.e. Clifford+T). Although our implementation of synthesis by diagonalization uses RL, other search-based synthesis methods are equally valid. A tool such as Synthetiq can be retrofitted to leverage diagonalization.

### 3.1 Handling Diagonal Unitaries and Rotation Gates

The diagonal operator  $D_\theta$  captures continuous degrees of freedom that cannot be efficiently handled by the  $L_t$  and  $R_t$  unitaries. An ansatz implementing  $D_\theta$  can be prepared using specialized algorithms for synthesizing diagonal unitaries [9, 31, 54]. These diagonal unitaries require only *CNOT* and  $R_Z$  gates. In this paper,  $R_Z$  rotations are implemented without ancilla in the Clifford+T gate set using *gridsynth* [43], but alternative techniques can also be used.

## 4 Reinforcement Learning with Unitaries

To diagonalize unitaries, we adopt a Reinforcement Learning approach called the Diagonalizing Value Network for Unitaries (DVNU). DVNU indirectly learns a diagonalization policy  $\pi$  using Value Iteration [4]. Compared to the approaches described in [11, 34], our model-based method trains faster and achieves better synthesis performance.

We introduce advancements necessary for compiling more complex quantum programs. First, we introduce a global phase invariance operation. Invariance to global phase ensures that networks learn to associate values with a canonical form of a unitary state. Second, we introduce a unitary perturbation data augmentation. By applying small unitary disturbances to states during training, the network learns to associate values with regions centered around points on the Bloch sphere. The impact of these architectural changes are illustrated in Figure 6. An ablation study summarizes the effect on performance of all architectural changes (see Figure 8). These improvements to the neural network architecture are evaluated only on discrete gate synthesis tasks, but are likely to boost performance in other problem domains such as parameterized ansatz search and seeded synthesis [53].

### 4.1 Modeling Synthesis

Our search-based synthesis method relies on a form of RL called *model*-based learning.

*Definition 4.1.* A *model* is a function  $f$  which predicts the dynamics of a controllable environment  $f(s_t, a_t) = \tilde{s}_{t+1}$ .

In the case of quantum circuit synthesis, knowledge of the state  $s_t$  and the action  $a_t$  allows for exact, deterministic, knowledge of the system dynamics because  $s_{t+1} = a_t \times s_t$  or  $s_{t+1} = s_t \times a_t$ .

### 4.2 A Global Phase Invariant Network Architecture

Two observables which differ only by a global phase cannot be distinguished experimentally [35]. When dealing with unitary operators numerically, we are forced to choose representations which may differ due to global phase. To ensure that equivalent unitaries are represented in the same way, we require global phase invariance.

*Definition 4.2.* A function  $g$  is said to be *global phase invariant* if for two unitaries  $U, W \in \mathbb{U}(2^n)$  and  $\theta \in \mathbb{R}$  such that  $U = e^{i\theta}W$ , it is the case that  $g(U) = g(W)$ .

We construct a new phase invariant neural network layer similar to the manner of [47], which showed how nonlinear activation functions may be made equivariant to complex phase. Figure 5 illustrates this process and a proof of its correctness can be found in the Appendix.

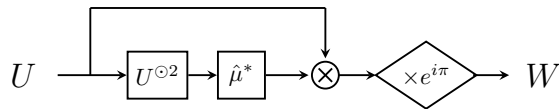


Fig. 5. A unitary  $U$  can be transformed to global phase invariant representation  $W$  by 1) squaring  $U$  element-wise, 2) computing and conjugating the normalized mean to obtain a unit magnitude complex number  $\hat{\mu}^*$ , 3) multiplying  $\hat{\mu}^* \times U$ , and 4) conditionally correcting the phase by an angle of  $\pi$ . The Appendix contains further details.

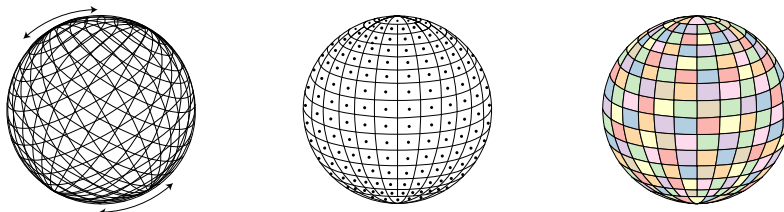


Fig. 6. Visualization of global phase invariance and unitary perturbative data augmentations. Points on the *Bloch sphere* represent pure single-qubit quantum mechanical state vectors [35]. *Left*: Without global phase invariance, the Bloch sphere is rotated so that equivalent quantum states have different representations. *Center*: With no unitary perturbations on the inputs, reachable quantum states are only represented as single points. *Right*: Global phase invariance and unitary perturbations ensure that quantum states are represented consistently and that the network learns to associate entire  $\epsilon$ -regions with values.

### 4.3 Unitary Perturbations for Robust Value Learning

Unitary synthesis constructs approximate implementations of unitaries. As indicated by the distance condition in Equation 2, each unitary is associated with an  $\epsilon$ -disk of unitaries which are considered to be approximately equivalent. This fact naturally inspires a perturbative data augmentation technique: small unitary disturbances are applied to unitary states in order to learn this approximate equivalence structure.

Concretely, given a unitary state  $s_t$ , a unitary perturbation  $U_\epsilon$  satisfying  $d_{HS}(U_\epsilon, I) < \epsilon$  is applied so that the state viewed by the agent is  $U_\epsilon \times s_t$  (or  $s_t \times U_\epsilon$ ). A visualization of the unitary perturbation data augmentation is illustrated in Figure 6. The impact on performance is depicted in Figure 8.

### 4.4 Neural Radiance Field Encoding

Unitary states are represented using  $2 \times 2^n \times 2^n$  real tensors, where  $n$  is the number of qubits. As we focus only on cases of high-precision synthesis where  $n \in \{1, 2, 3\}$ , our input data is extremely information dense. Past work has shown that neural networks struggle to fit high frequency patterns in data [40, 55]. We adopt a positional encoding technique used widely in the field of novel view synthesis and introduced by the NeRF project [32]. Input values are transformed by a map  $\gamma : \mathbb{R} \rightarrow \mathbb{R}^{2L}$  such that

$$\gamma(x_i) = \left( \sin(2^0 \pi x_i), \cos(2^0 \pi x_i), \dots, \sin(2^{L-1} \pi x_i), \cos(2^{L-1} \pi x_i) \right) \quad (9)$$

This encoding map plays a vital role in allowing networks to detect small magnitude differences in each element of a unitary state. The encoding therefore transforms input tensors from a shape of  $(2, 2^n, 2^n)$  to a shape of  $(2, 2^n, 2^n, 2L)$ . For our experiments, we set  $L = 15$ .

#### 4.5 Diagonalizing Value Network for Unitary Synthesis

We leverage deep value iteration to learn gate set specific value functions. We refer to this architecture as the Diagonalizing Value Network for Unitaries (DVNU). This contrasts with past work such as [11, 34] which leverage Deep Q Networks (DQN) [33]. To train a DQN agent, a state-action value (Equation 4) must be learned for *each*  $(s_t, a_t)$  pair. To ensure adequate training, the agent must receive examples of many different actions taken in each state. When the number of actions (in this case the gate set  $|A|$ ) is large, the sample inefficiency of the DQN algorithm limits training progress. In comparison, the DVNU agent must only learn the value of a state  $s_t$ . The policy used is

$$\pi(a|s_t) = \arg \max_{a \in A} V_{\theta}^{\pi}(a \times s_t) \quad (10)$$

Value iteration [50] is possible because synthesis can be modeled exactly and the reward is a deterministic function of the state. The previous work of [57] also employed a method based on value iteration for topological quantum computing. More recently [1] demonstrated how in restricted cases, tabular (as opposed to deep RL) policy iteration can be used to solve for optimal synthesis policies.

### 5 Experiments

In this section we evaluate our Reinforcement Learning diagonalization approach to quantum circuit synthesis detailed in Section 4. As inputs we consider randomly generated unitaries together with unitaries extracted from a collection of algorithms/programs used in many other synthesis studies. We show how our method can synthesize high-precision unitaries which are out of reach for other synthesis approaches.

A direct comparison of FT synthesis algorithms is complicated due to the trade-offs and intricacies of each method. At high levels of precision, most synthesis algorithms fail to find solutions. As a baseline, we consider the general approach where circuits are synthesized analytically using the Quantum Shannon Decomposition, followed by single-qubit FT synthesis of  $R_Z$  gates. This is compared against our method applied to two and three qubit unitaries extracted from a number of benchmark circuits.

#### 5.1 The Impact of Global Phase Invariance and Perturbations

How do the proposed neural architectural modifications proposed in Section 4 impact performance? To answer this question, we can compare the ability of invariant and non-invariant architectures to learn useful properties about unitaries. We take as a proxy task the problem of predicting which unitary is associated with which gate in a finite gate set. Two structurally identical multi-layer perceptron [42] networks are trained to assign gate labels to unitaries associated with the two-qubit Clifford+T gate set for 250 epochs. Figure 7 illustrates how the network which first applies the invariance operation detailed in Section 4.2 is resilient to global phase disturbances; no matter the global phase shift it is able to correctly match unitaries with their associated gates.

Global-phase invariance enables neural networks which operate on quantum datasets to achieve better performance. Actively addressing this symmetry removes the requirement that networks learn invariant representations. In the 1-qubit case, the impact of global-phase invariance is less evident; agents trained with and without dephasing achieve similar performance. The effect is more pronounced when tackling 3-qubit circuit synthesis (see Figure 8). The impact of the unitary perturbation data augmentation technique, and the advantage of using NeRF encodings, are both evident even when synthesizing single-qubit unitaries.

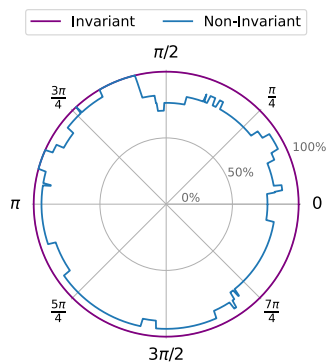


Fig. 7. Accuracy of global phase invariant and non-invariant architectures as a function of phase shift. Two otherwise identical networks are trained to match unitaries with their associated Clifford+T gates. Global phase shifts (angles on the unit circle) are applied to unitaries during training and testing. The *invariant* architecture maintains perfect accuracy (keeps a radius of 100%); it correctly matches unitaries with their associated gate no matter the global phase.

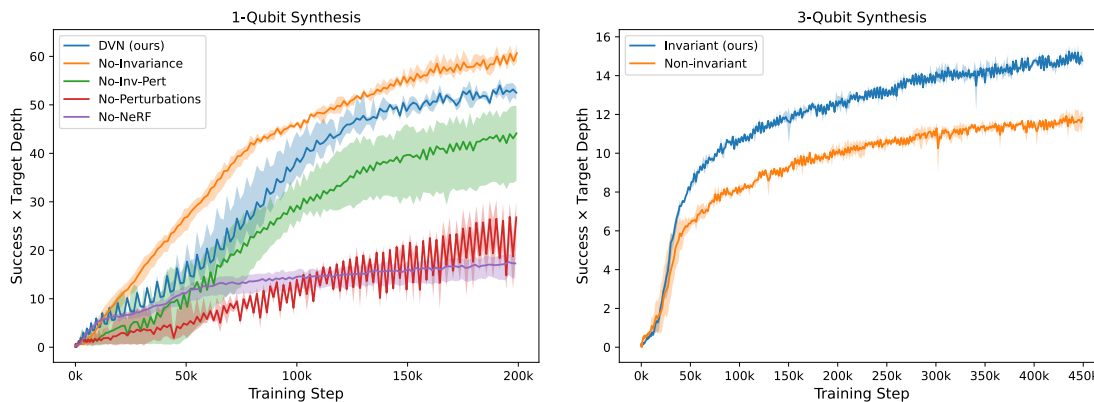


Fig. 8. Ablation study for 1-qubit (left) and 3-qubit (right) synthesis. Lines are the mean of four runs, shaded regions depict extrema. The *y*-axis scales agent success given a problem instance’s difficulty. Global phase invariance can be learned in the simplest cases (1-qubit synthesis), but is necessary for harder problems (2- and 3-qubit synthesis). Invariant architectures outperform non-invariant ones given enough training time.

## 5.2 Evaluating DVNU Against Other RL Approaches

For this experiment, random unitary targets are obtained by randomly generating quantum circuits in the Clifford+T gate set consisting of  $\{H, X, Y, Z, S, T, S^\dagger, T^\dagger\}$  gates. Circuits are generated by randomly selecting a member of the 1-qubit Clifford group followed by either  $T$  or  $T^\dagger$ . Random circuits are used during training because they can easily be generated and because the difficulty of synthesizing the unitaries associated with these circuits can be tuned by adding or removing gates. Agents in this experiment are trained to invert unitaries, meaning that the state representation used is  $s_t = L_t U_{tar}^\dagger I_2^n$ , and the distance function used is the Hilbert Schmidt distance (Eq 2).

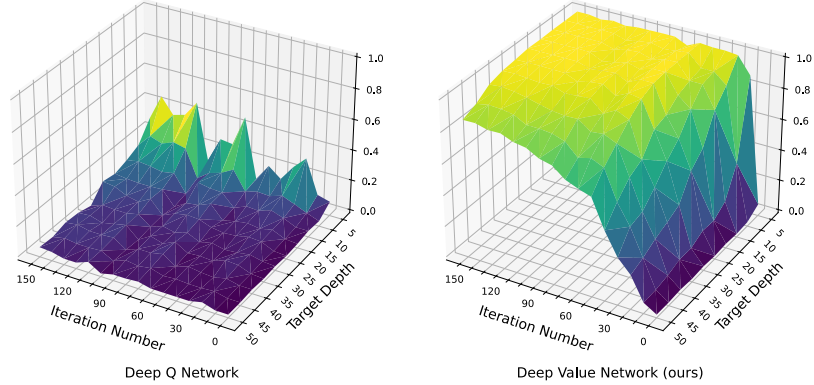


Fig. 9. Probability that a DQN agent (left) and a DVNU agent (right) successfully finds implementations of random 1-qubit Clifford+T unitaries by inversion. The DQN learns a Q function (Eq 4) whereas the DVNU agent learns a value function (Eq 3). The *Target Depth*-axis shows the number of gates in 250 randomly generated compilation targets. Adding gates increases compilation difficulty. The *Iteration Number*-axis measures how much training time has passed. The vertical axis shows the probability that a compilation agent will successfully compile a target circuit. The architectural modifications made to the DVNU agent improve upon previously demonstrated state-of-the-art deep-learning-based unitary synthesis approaches.

The metric of interest here is the likelihood that a discrete gate synthesis algorithm finds a circuit implementation of a target unitary. There are  $O(|A|^d)$  depth  $d$  possible circuits to check, so performance on this task estimates how well an agent has learned to navigate this huge state space.

We train two models, a DQN (which learns a Q function) as in [34] and a DVNU (which learns a value function). Both networks were made invariant to global phase. Agents are trained for 150 iterations (about 6 hours) on a machine with an AMD EPYC 7763 CPU and an NVidia A100 GPU. Figure 9 illustrates the results of this experiment. After training, the 1-qubit DVNU agent was able to synthesize random Clifford+T circuits of depth 80 with a success rate of 54%. Comparisons to other RL synthesis projects are highlighted in Table 1.

Given the same time budget, the DVNU agent achieves higher synthesis performance across all evaluated problem difficulties. This can partially be explained by the greater sample efficiency of value iteration compared to Q learning. By leveraging a deterministic and exact model of synthesis, values are associated with states instead of state-action pairs.

### 5.3 Comparing DVNU Synthesis to the Quantum Shannon Decomposition

Given a 2-3 qubit target, we wish to determine how well the DVNU-based Reinforcement Learning diagonalization approach can synthesize unitaries. Throughout these experiments, we require that unitaries be synthesized to a distance of  $\epsilon = 10^{-6}$  (see Equation 2). In many cases, the diagonalizing agent produces far more precise circuit implementations of unitaries. In Section 5.4, we synthesize unitaries to an even higher precision. At this value of  $\epsilon$  pure search-based tools are unable to synthesize unitaries by inversion. To test this assertion, we attempted to synthesize our suite of unitaries with Synthetiq: a simulated annealing tool which empirically achieves state-of-the-art performance [37]. Because Synthetiq attempts to invert matrices, many targets remain out of reach. Solutions could only be found within a 20 minute time out period when inputs contained no continuous rotations (i.e.  $U_3$  or  $R_Z$  gates).

		Heisenberg	HHL	Hubbard	QAOA	QPE	Shor	TFIM	VQE	Mean
2 Qubits	Time per Unitary (s)	0.98	0.96	0.97	0.98	0.97	0.96	0.98	0.96	0.97
		0.93	0.63	0.92	0.86	0.59	0.73	0.52	0.87	0.76
	Success Rate	100%	100%	100%	100%	100%	100%	100%	100%	100%
		93.7%	37.4%	42.8%	27.1%	29.1%	41.7%	51.0%	20.0%	42.9%
	$R_Z$ Count	7.07	7.58	6.34	8.27	7.88	7.31	6.15	4.88	6.94
		1.0	1.64	0.85	1.06	0.91	1.56	1.0	0.94	1.12
	T Count	0.28	0.29	0.04	0.42	0.22	0.15	0.00	0.02	0.18
	0.03	0.36	0.00	0.00	1.15	0.10	0.00	0.16	0.23	
Clifford Count	4.66	4.20	4.63	5.15	4.35	5.77	2.06	3.33	4.27	
	4.39	4.01	3.16	2.10	3.50	4.07	5.47	8.31	4.38	
Non-Clifford Reduction	<b>85.9%</b>	<b>78.4%</b>	<b>86.6%</b>	<b>87.2%</b>	<b>88.5%</b>	<b>78.7%</b>	<b>83.7%</b>	<b>80.7%</b>	<b>83.5%</b>	
3 Qubits	Time per Unitary (s)	1.07	1.06	1.06	1.18	1.07	1.18	1.07	1.05	1.09
		1.03	1.07	1.12	1.02	1.06	1.12	1.01	0.98	1.05
	Success Rate	100%	100%	100%	100%	100%	100%	100%	100%	100%
		27.4%	9.6%	55.6%	11.2%	78.5%	18.0%	9.4%	13.3%	27.9%
	$R_Z$ Count	44.60	30.42	36.73	30.96	46.89	43.67	34.63	43.57	38.93
		1.88	2.06	0.87	2.27	1.48	4.21	1.90	0.72	1.92
	T Count	1.46	0.68	1.85	1.22	1.26	1.80	1.10	1.84	1.40
	0.10	2.15	0.47	0.00	3.54	0.28	0.17	0.43	0.89	
Clifford Count	33.85	29.24	34.48	30.06	35.41	37.95	29.95	34.96	33.24	
	13.06	15.94	14.85	10.22	14.00	11.92	16.76	16.69	14.18	
Non-Clifford Reduction	<b>95.8%</b>	<b>93.2%</b>	<b>97.6%</b>	<b>92.7%</b>	<b>96.8%</b>	<b>90.4%</b>	<b>94.5%</b>	<b>98.3%</b>	<b>95.1%</b>	

Table 2. Synthesis of 2- and 3-qubit unitaries taken from partitioned circuits (see Figure 10 for an illustration). Numbers indicate average time, success rate, Clifford, and non-Clifford gate counts for unitaries taken from a variety of benchmarks. Compared to the QSD (top rows), the diagonalizing agent (bottom rows) on average reduces the number of  $R_Z$  gates by 83.5% and 95.1% for 2- and 3-qubit unitaries respectively. Comparisons are made to the QSD because other synthesis tools fail to find solutions given  $\epsilon \leq 10^{-4}$ .

As a point of reference, we compare synthesis results of the diagonalizing agent to the Quantum Shannon Decomposition (QSD) [44]. This analytical decomposition was chosen because no other search-based tool that we tested was able to find solutions with sufficient precision. Results from the QSD are optimized by converting and combining  $R_Z$  gates into Clifford+T gates when possible.

To train the DVNU diagonalizing agent, we randomly generated separate  $A$  and  $B$  Clifford+T circuits, then inserted random  $R_Z$  rotations to form targets in the form  $AR_Z^{\otimes n}(\theta_i)B$ . In the 2- (3-)qubit case, the  $A$  and  $B$  circuits contained up to a combined 30 (20) gates.

We evaluated the diagonalizing agent’s performance on a set of unitaries taken from partitioned quantum algorithms (see Figure 10 for an illustration of how circuits are partitioned). This suite of algorithms includes Shor’s Algorithm [46], TFIM, Heisenberg, and Hubbard model quantum chemistry simulation circuits [3], trained VQE [38] and QAOA [18] circuits, and Quantum Phase Estimation circuits [26]. The VQE and QAOA circuits were generated by MQTBench [39]. Each set of unitaries was filtered to ensure that every unitary was unique. There were 22,323 different 2-qubit unitaries and 45,202 different 3-qubit unitaries. Table 2 summarizes.

Unitaries which are diagonal, or nearly diagonal, are ubiquitous primitives in realistic quantum benchmarks. These common unitaries are nearly trivial to synthesize under the diagonalizing approach, but often are out of reach for inversion-based synthesis algorithms. The Toffoli gate (which is synthesized with optimal ancilla-free T-count and illustrated in Figure 4) and  $CCR(\theta)$  gates are examples of commonplace, nearly diagonal, unitaries.

We find that in the two-qubit case, diagonalization can find circuits implementing 42.9% of unitaries across all benchmarks. About 79% of these unitaries are already diagonal, and therefore trivial for a diagonalizing agent to synthesize. Most other unitaries contain 2-8 gates, typically single-qubit Hadamard and S gates.

For the three-qubit case, realistic unitaries are far more complex: they are more likely to contain unitaries which do not conform to the diagonalization ansatz (see Figure 4). Approximately 27.9% of three-qubit unitaries from our suite of partitioned circuits could be synthesized by the diagonalizing agent. Of these, approximately 57% were already diagonal. On average, 3.84 CNOT gates are needed to implement the diagonal operator, meaning the diagonalizing DVNU agent typically finds diagonalizing  $L_t(\cdot)R_t$  implementations with an average of about 11 Clifford+T gates.

Compared to the QSD, the diagonalizing agent produces solutions with far fewer non-trivial rotation gates. Implementing an  $R_Z$  gate requires  $O(\log \frac{1}{\epsilon})$  T gates when synthesized optimally with *gridsynth* [43]. For  $\epsilon = 10^{-6}$  this is approximately 60 T gates per  $R_Z$ . Lone T gates are almost negligible compared to continuous rotations in the high precision regime. Compared to the QSD, the DVNU synthesizer reduces the average number of non-Clifford gates by 83.5% for two qubit unitaries and 95.1% for three qubit unitaries.

Although the success rate for the DVNU agent is lower than for mathematical decompositions, the potential savings in non-Clifford gates and the speed with the process runs remain strong arguments for its utility. Next, we demonstrate how the DVNU approach to synthesis can be used to transpile future-term quantum algorithms into the Clifford+T gate set.

#### 5.4 A Fault-Tolerant Circuit Synthesis Workflow

Unitary synthesis algorithms are well suited for transpiling quantum circuits into new sets of gates. Past work [56] targeting NISQ gates has demonstrated how multi-qubit synthesis techniques can produce implementations of higher quality than when using optimal single- and two-qubit [51] synthesis. In this scenario, the additional optimization power comes from replacing gate-by-gate local optimization with more global optimization of multi-qubit unitaries.

Our DVNU agent is able to find solutions to a far more general set of unitaries at high precision than the current state-of-the-art methods. The question remains whether in the FT case techniques that are able to handle complex unitaries are better than composing optimal techniques for simple (lower dimension) unitaries.

To demonstrate how diagonalization can be leveraged to transpile algorithms into FT gate sets with synthesis we compare the results of multi-qubit FT synthesis to that of *gate-level* transpilation; where circuits are transpiled gate-by-gate (as opposed to subcircuit-by-subcircuit) into the Clifford+T gate set. This strategy is used as a point of comparison for the DVNU agent because the only other methods that produce high precision implementations of these unitaries, the QSD, results in  $O(4^n)$  T gates (Table 2).

A high level summary of the process used is shown in Figure 10. For 3-qubit synthesis, our method is as follows:

- (1) Partition a quantum circuit into 3-qubit blocks that contain as many gates as possible.
- (2) For each 3-qubit unitary, use the DVNU agent to generate a high precision approximation using diagonalization.
- (3) If DVNU fails to synthesize a unitary, split it into 2-qubit unitaries and again attempt synthesis.
- (4) For all unitaries that still do not meet the threshold, take the original partitioned subcircuit and convert single-qubit parameterized gates into a sequence of  $R_Z$  and Clifford gates. Use gate replacement rules for other non-Clifford+T gates.
- (5) Decompose  $R_Z$  gates with *gridsynth* produced Clifford+T sequences.

Table 3 summarizes these results across several quantum algorithms and primitives. The total approximation error  $\epsilon$  across the entire circuit is on the order of  $10^{-6}$ . This value is an upper bound that is found by summing the individual

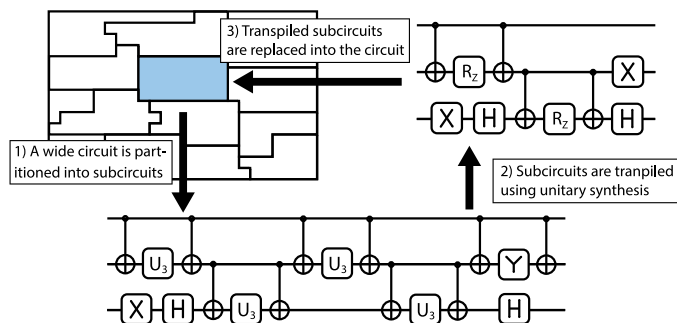


Fig. 10. Fault-Tolerant gate set transpilation using unitary synthesis. Quantum algorithms are partitioned into many subcircuits. These subcircuits are transpiled independently using unitary synthesis. The optimized and transpiled subcircuits are then replaced into the original circuit.  $R_z$  gates are handled in a post-processing stage using *gridsynth*.

	Qubits	Add	HHL	Mult	QAE	QFT	QPE	Shor
By Gate	$T$ Gates	22,646	21,977	97,250	60,750	97,231	28,890	73,446
	Cliffords	35,404	34,243	152,188	97,048	152,375	45,867	117,492
	$\epsilon_{\text{total}}$	$0.3 \times 10^{-6}$	$0.2 \times 10^{-6}$	$1.1 \times 10^{-6}$	$0.7 \times 10^{-6}$	$1.1 \times 10^{-6}$	$0.3 \times 10^{-6}$	$0.8 \times 10^{-6}$
2Q Blocks	$T$ Gates	21,656	21,797	97,250	58,014	97,232	27,987	74,446
	Cliffords	33,867	34,194	152,188	92,675	152,268	44,348	117,492
	$\epsilon_{\text{total}}$	$0.6 \times 10^{-6}$	$0.3 \times 10^{-6}$	$1.2 \times 10^{-6}$	$4.8 \times 10^{-6}$	$4.4 \times 10^{-6}$	$1.1 \times 10^{-6}$	$0.8 \times 10^{-6}$
	% Diagonalized	94.0%	72.4%	92.7%	45.1%	91.0%	21.4%	26.2%
	Improvement	4.4%	0.8%	0%	4.5%	0%	3.1%	0%
3Q Blocks	$T$ Gates	19,489	21,707	80,935	59,760	85,441	28,440	73,446
	Cliffords	30,748	33,857	127,048	96,999	135,051	45,361	117,492
	$\epsilon_{\text{total}}$	$0.4 \times 10^{-6}$	$0.3 \times 10^{-6}$	$1.2 \times 10^{-6}$	$4.2 \times 10^{-6}$	$3.1 \times 10^{-6}$	$1.0 \times 10^{-6}$	$0.8 \times 10^{-6}$
	% Diagonalized	85.1%	14.3%	73.5%	40.6%	85.3%	14.4%	12.5%
	Improvement	13.9%	1.2%	16.8%	1.6%	12.1%	1.6%	0%

Table 3. Transpilation results. The *By Gate* strategy indicates gate-level transpilation into Clifford+ $T$  gates. The *2Q* and *3Q Block* strategies indicate circuits partitioned into subcircuits of that size and synthesized by diagonalization. In scenarios where diagonalization fails, subcircuits are transpiled gate by gate. Each subcircuit is synthesized to a distance of  $\epsilon = 10^{-8}$ . Individual  $R_z$  gates are synthesized to  $\epsilon = 10^{-9}$ , resulting in at least 90  $T$  gates per  $R_z$ . The total approximation error in each circuit on the order of  $\epsilon_{\text{total}} \approx 10^{-6}$ .

approximation errors for each partition and each *gridsynth* transpiled  $R_z$  gate [52]. Transpilation via diagonalization results in savings in the number of  $T$  gates needed for these algorithms compared to the gate-level transpilation strategy. We see the highest  $T$  gate count reduction (16.8%) for the 16 qubit multiplier circuit. Other algorithmic primitives such as the 17 qubit adder circuit, and the 32 qubit QFT see similarly large reductions. The HHL, QAE, and QPE circuits see more moderate decreases in  $T$  count.

The performance of the diagonalizing agent for transpilation is highly dependent on the circuit partitioning algorithm, which in this case is driven by circuit structure. For example, a 16-qubit implementation of Shor’s algorithm sees no

improvement when using diagonalization compared to the gate-level transpilation strategy. The 2-qubit diagonalizing agent is only able to find transpiled implementations to 26% of unitaries taken from this circuit. We likewise observe that only 12% of partitioned 3-qubit subcircuits are diagonalized for this same circuit. Shor’s algorithm consists of many repeated copies QFT and inverse QFT modules, which we know can be simplified well with diagonalization. For 2- and 3-qubit partitions, 91% and 85% of subcircuits taken from the example QFT circuit can be transpiled by the DVNU agent. This indicates that performance of FT transpilation algorithms which leverage synthesis are highly dependent on the partitioning algorithm used.

Combined with circuit partitioning, unitary synthesis enables transpilation to take place on a less localized scale. This more global view of a circuit’s function allows for synthesis to outperform simple gate-level rule-based methods.

## 6 Discussion

Resource efficient transpilation into FT gate sets is vital for practical quantum error corrected computation. To this end, high precision synthesis targeting the Clifford+T gate set is a invaluable asset. Here, we discuss how diagonalization-based synthesis with DVNU can be further developed in pursuit of this goal.

### 6.1 Trade-Offs for High Precision Synthesis of Realistic Unitaries

In order to be useful for large scale FT computation, synthesis algorithms must be able to approximate unitaries to high levels of precision. In the worst case, the total approximation error in a transpiled circuit is the sum of each individual gate’s or partition’s approximation error [52]. If the circuits transpiled in Section 5.4 (see Table 3) had instead been handled by a synthesis algorithm capable of only finding solutions to a precision of  $\epsilon = 10^{-3}$ , the average total approximation error of the transpiled circuits would be upper bounded by  $\epsilon_{\text{total}} = 0.56$  (ranging from 0.05 to the maximum error of 1.0). This amount of approximation error is unlikely to lead to meaningful algorithm outputs. The outlook for coarse synthesis is even worse for larger width circuits.

Because diagonalization allows for  $2^n - 1$  continuous rotations to be handled analytically, much higher levels of precision are possible with this approach. In fact, we can consider the class of *exactly diagonalizable* unitaries (analogous to exactly synthesizable unitaries), where  $U = RD_{\theta}^{-1}L$  and each entry of  $L, R \in \mathbb{Z}[e^{i\pi/4}, \frac{1}{2}]$ . These exactly diagonalizable unitaries can be approximated to arbitrarily high levels of precision using synthesis by diagonalization, so long as implementations can be found for  $L$  and  $R$ . Common examples of these unitaries include those that can be constructed with sequences of controlled rotation gates  $CR(\theta)$ .

We have demonstrated how our Reinforcement-Learning-based diagonalization approach can synthesize realistic unitaries to precisions between  $\epsilon = 10^{-6}$ - $10^{-8}$ . These values are orders of magnitude ( $10^3$ - $10^5\times$ ) more precise than previous methods (see Table 1) and enable high precision transpilation of complete algorithms (see Table 3). Determining the exact precision needed to ensure circuits produce meaningful results is an open area of research in both NISQ and FT domains. The precision attainable using the diagonalization framework can also be boosted with advanced techniques such as unitary mixing [10]. This entails compiling multiple unique gate sequences which approximately implement a given continuous  $R_Z$  rotation. These different gate sequences should be used over the course of multiple executions of an algorithm.

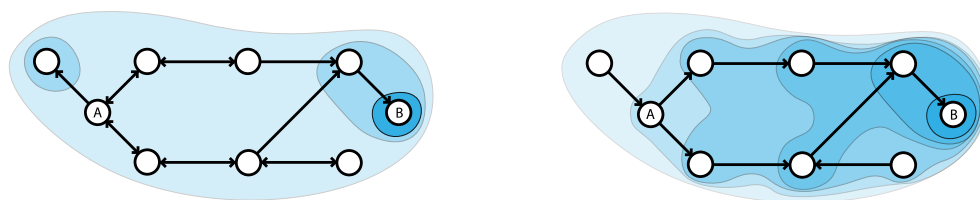
No matter the end-precision required, this work showcases the benefit of augmenting analytical decomposition methods (which result in many non-Clifford gates) with search-based multi-qubit methods. Although diagonalization produces higher quality results than pure analytical decompositions, these results are likely non-optimal in non-Clifford

gate counts. We expect that other analytical-search-based hybrid approaches that offer further improvements are both possible and practical.

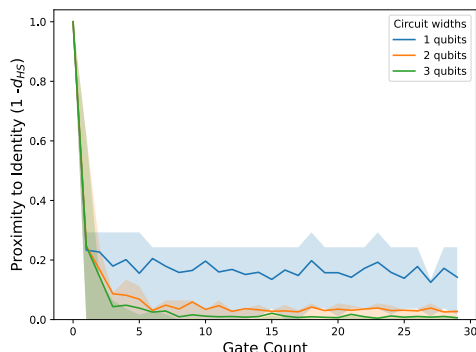
### 6.2 Interpreting the Value Function

In order for a function to meaningfully guide search-based synthesis, it should correlate with the goal of finding short gate count implementations of unitaries. Intuitively, the value of a synthesis state should depend on the number of gates needed to transform that state into a terminal state.

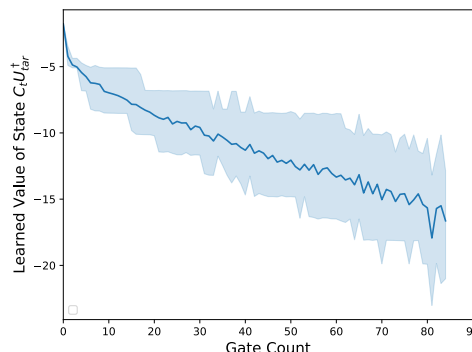
A discrete gate set synthesis algorithm which relies directly on the Hilbert-Schmidt distance function (or Frobenius norm, diamond norm, etc.) to guide the placement of gates will randomly search the space of possible circuits. Many synthesis algorithms to date use these cost functions to guide gate placement [14, 37, 49]. Figure 11c shows how for random Clifford+T circuits, Hilbert-Schmidt distance does not correlate strongly with the number of gates in the circuit (and therefore the number of gates needed to synthesize that unitary). Synthesis states in the neighborhood of the current state appear equally distant from a terminal state.



(a) State transition diagram under a noisy and flat value function. (b) State transition diagram under the learned value function.



(c) Proximity to the identity ( $1 - d_{HS}(s_t, I)$ ) vs. gate count of random Clifford+T circuits. This value function is noisy and flat, causing agents to act randomly in most of the state space.



(d) Learned value of synthesis states vs. gate count of random single qubit Clifford+T circuits. This value function guides agents towards terminal states.

Fig. 11. The impact of the value function on state transitions. (a) Agents which use noisy and flat value functions to plan actions will act randomly. Nodes *A* and *B* represent the initial and terminal states respectively. Darker contours represent increasing value magnitudes. (b) Agents which use learned values to plan actions tend towards terminal states. (c) shows the Hilbert-Schmidt distance which is a noisy and flat value function. Lines are the mean distances of 250 random circuits, the shaded regions are interquartile ranges. In synthesis with discrete gate sets, unitary distance does not correlate with gate count. States which require fewer gates to reach a terminal state generally do not correspond to lower distances than states which require more gates. (d) shows the learned value function which is based on path distance. States which require fewer gates to reach a terminal state have higher values than those which require more gates. Gate cancellation in randomly generated circuits contributes to variance in state values.

*How does a Reinforcement Learning agent avoid this pitfall?* Under a reward function such as Equation 7, the learned value of states correlates with the number of gates in the circuit. As shown in Figure 11d, the value of a state is a *learned, scaled and, shifted* representation of the *gates to go*. This property makes the agent a fast and efficient synthesizer; it ideally takes the shortest direct path to a terminal state.

In the case of exact synthesis of single-qubit Clifford+T unitaries, the *smallest divisor exponent* (SDE) plays a similar role as the value function [28]. This synthesis algorithm sequentially takes actions depending on which gate decreases the SDE. In the multi-qubit case, it is believed that such a simple function does not naturally exist [22]. The model-based RL approach taken in this paper can be construed as a learned version of the SDE function for approximate multi-qubit synthesis.

### 6.3 The Utility of Diagonalization for Compilation Tasks

By augmenting search-based compilation with generalized analytical decomposition, our DVNU agent is able to greatly expand the domain of unitaries that can be transpiled and increases the precision to which they are transpiled. However, diagonalization also enables even more powerful compilation strategies.

The use of ancilla qubits and projective measurements exposes more opportunity for optimization when implementing operations in FT gate sets. Probabilistic Quantum Circuits with Fallback [6] and Repeat Until Success [7] schemes leverage these resources to reduce the number of non-Clifford gates needed to implement  $R_Z$  rotations compared to optimal ancilla-free synthesis. These techniques rely on synthesizing unitaries with a particular structure (the so called *Jack of Daggers* structure). As a powerful synthesis approach, diagonalization can be used to explore other structures which can systematically decrease non-Clifford gate counts when paired with ancilla.

By loosening the synthesis objective from inversion to diagonalization, our tool also exposes opportunity for resource-efficient implementations of continuous rotations. [12] leverages phase kickback and adder circuits to express single-qubit  $Z$ -axis rotations much more efficiently than a standard gate decomposition. Our technique naturally finds multi-qubit  $Z$ -axis rotations (diagonal unitaries). It may be possible to combine these techniques to more efficiently approximate complex continuous rotations across multiple qubits.

As most FT synthesis work has focused on the Clifford+T gate set, there may be unexplored optimization opportunity when considering alternate gate sets such as Clifford+ $\sqrt{T}$  and Clifford+V. Search-based synthesis tools are well suited to begin answering these questions, as synthesis in alternative gate sets is simply a matter of modifying the set of actions an agent can apply.

## 7 Conclusion

We have demonstrated a novel approach to high precision unitary synthesis targeting fault-tolerant gate sets. By diagonalizing unitaries instead of directly inverting them, complex continuous degrees of freedom can be avoided then handled efficiently using mathematical decomposition methods. This enables us to synthesize a broader scope of unitaries than other search-based synthesis methods which directly invert continuous rotations, a task which is intractable for high levels of precision. The diagonalization process is general and other synthesis tools can be retrofitted to diagonalize rather than invert unitaries.

We also developed novel operations which can be applied to neural network architectures: global phase invariance and unitary perturbations. These modifications enable deep learning to more effectively learn on datasets of unitary matrices. The effectiveness of our Diagonalizing Value Network for Unitaries (DVNU) Reinforcement-Learning-based approach is demonstrated by synthesizing unitaries taken from a suite of partitioned quantum algorithms to very high

precision. In this regime, only resource inefficient analytical methods are also able to find solutions. Compared to the Quantum Shannon Decomposition, our approach reduces the number of expensive  $R_Z$  rotations (and therefore T-gates) by 83.5% in two-qubit unitaries and 95.1% in three-qubit unitaries. We demonstrate how our approach can be used to transpile future-term algorithms to fault-tolerant gate sets with very low approximation error. Using DVNU for transpilation results in up to a 16.8% reduction in non-Clifford gates for these algorithms. Our diagonalizing approach is fast and able to find low gate count implementations of meaningful unitaries, making it a promising technique for use in future fault-tolerant quantum compilers.

## Acknowledgments

The authors thank Samuel Pfrommer for useful discussion about NeRF encodings. This work was supported by the DOE under contract DE-5AC02-05CH11231 through the Office of Advanced Scientific Computing Research (ASCR) Quantum Algorithms Team and Accelerated Research in Quantum Computing programs. This work was also supported by the NSF Challenge Institute for Quantum Computation (CIQC) program under award OMA-2016245 and through a CIQC seed funding award.

## References

- [1] M. Sohaib Alam, Noah F. Berthussen, and Peter P. Orth. 2023. Quantum logic gate synthesis as a Markov decision process. *npj Quantum Information* 9, 1 (10 2023). <https://doi.org/10.1038/s41534-023-00766-w>
- [2] Matthew Amy, Dmitri Maslov, Michele Mosca, and Martin Roetteler. 2013. A meet-in-the-middle algorithm for fast synthesis of depth-optimal quantum circuits. *IEEE Transactions on Computer-Aided Design of Integrated Circuits and Systems* 32, 6 (June 2013), 818–830. <https://doi.org/10.1109/TCAD.2013.2244643> arXiv:1206.0758 [quant-ph].
- [3] Lindsay Bassman, Connor Powers, and Wibe A. De Jong. 2022. ArQTic: A Full-Stack Software Package for Simulating Materials on Quantum Computers. *ACM Transactions on Quantum Computing* 3, 3, Article 17 (jul 2022), 17 pages. <https://doi.org/10.1145/3511715>
- [4] Richard Bellman. 1957. *Dynamic Programming* (1 ed.). Princeton University Press, Princeton, NJ, USA.
- [5] Dolev Bluvstein, Simon J. Evered, Alexandra A. Geim, Sophie H. Li, Hengyun Zhou, Tom Manovitz, Sepehr Ebadi, Madelyn Cain, Marcin Kalinowski, Dominik Hangleiter, J. Pablo Bonilla Ataides, Nishad Maskara, Iris Cong, Xun Gao, Pedro Sales Rodriguez, Thomas Karolyshyn, Giulia Semeghini, Michael J. Gullans, Markus Greiner, Vladan Vuletić, and Mikhail D. Lukin. 2023. Logical quantum processor based on reconfigurable atom arrays. *Nature* 626, 7997 (Dec. 2023), 58–65. <https://doi.org/10.1038/s41586-023-06927-3>
- [6] Alex Bocharov, Martin Roetteler, and Krysta M. Svore. 2015. Efficient synthesis of probabilistic quantum circuits with fallback. *Physical Review A* 91, 5 (May 2015), 052317. <https://doi.org/10.1103/PhysRevA.91.052317> arXiv:1409.3552 [quant-ph].
- [7] Alex Bocharov, Martin Roetteler, and Krysta M. Svore. 2015. Efficient synthesis of universal Repeat-Until-Success circuits. *Physical Review Letters* 114, 8 (Feb. 2015), 080502. <https://doi.org/10.1103/PhysRevLett.114.080502> arXiv:1404.5320 [quant-ph].
- [8] Sergey Bravyi and Alexei Kitaev. 2005. Universal quantum computation with ideal Clifford gates and noisy ancillas. *Phys. Rev. A* 71 (Feb 2005), 022316. Issue 2. <https://doi.org/10.1103/PhysRevA.71.022316>
- [9] Stephen S. Bullock and Igor L. Markov. 2004. Asymptotically optimal circuits for arbitrary n-qubit diagonal comutations. *Quantum Info. Comput.* 4, 1 (jan 2004), 27–47.
- [10] Earl Campbell. 2017. Shorter gate sequences for quantum computing by mixing unitaries. *Physical Review A* 95, 4 (April 2017). <https://doi.org/10.1103/physreva.95.042306>
- [11] Qiu hao Chen, Yuxuan Du, Qi Zhao, Yuling Jiao, Xiliang Lu, and Xingyao Wu. 2022. Efficient and practical quantum compiler towards multi-qubit systems with deep reinforcement learning. arXiv:2204.06904 [quant-ph]
- [12] N Cody Jones, James D Whitfield, Peter L McMahon, Man-Hong Yung, Rodney Van Meter, Alán Aspuru-Guzik, and Yoshihisa Yamamoto. 2012. Faster quantum chemistry simulation on fault-tolerant quantum computers. *New Journal of Physics* 14, 11 (Nov. 2012), 115023. <https://doi.org/10.1088/1367-2630/14/11/115023>
- [13] M. P. da Silva, C. Ryan-Anderson, J. M. Bello-Rivas, A. Chernoguzov, J. M. Dreiling, C. Foltz, F. Frachon, J. P. Gaebler, T. M. Gatterman, L. Grans-Samuelsson, D. Hayes, N. Hewitt, J. Johansen, D. Lucchetti, M. Mills, S. A. Moses, B. Neyenhuis, A. Paz, J. Pino, P. Siegfried, J. Strabley, A. Sundaram, D. Tom, S. J. Wernli, M. Zanner, R. P. Stutz, and K. M. Svore. 2024. Demonstration of logical qubits and repeated error correction with better-than-physical error rates. arXiv:2404.02280 [quant-ph] <https://arxiv.org/abs/2404.02280>
- [14] Marc G. Davis, Ethan Smith, Ana Tudor, Koushik Sen, Irfan Siddiqi, and Costin Iancu. 2020. Towards Optimal Topology Aware Quantum Circuit Synthesis. In *2020 IEEE International Conference on Quantum Computing and Engineering (QCE)*. 223–234. <https://doi.org/10.1109/QCE49297.2020.00036>

- [15] A. De Vos and S. De Baerdemacker. 2016. Block-ZXZ synthesis of an arbitrary quantum circuit. *Phys. Rev. A* 94 (Nov 2016), 052317. Issue 5. <https://doi.org/10.1103/PhysRevA.94.052317>
- [16] Cirq Developers. 2024. *Cirq*. <https://doi.org/10.5281/zenodo.11398048>
- [17] Bryan Eastin and Emanuel Knill. 2009. Restrictions on Transversal Encoded Quantum Gate Sets. *Physical Review Letters* 102, 11 (March 2009). <https://doi.org/10.1103/physrevlett.102.110502>
- [18] Edward Farhi, Jeffrey Goldstone, and Sam Gutmann. 2014. A Quantum Approximate Optimization Algorithm. arXiv:1411.4028 [quant-ph] <https://arxiv.org/abs/1411.4028>
- [19] Austin G. Fowler, Matteo Mariantoni, John M. Martinis, and Andrew N. Cleland. 2012. Surface codes: Towards practical large-scale quantum computation. *Physical Review A* 86, 3 (Sept. 2012). <https://doi.org/10.1103/physreva.86.032324>
- [20] Vlad Gheorghiu, Michele Mosca, and Priyanka Mukhopadhyay. 2022. T-count and T-depth of any multi-qubit unitary. *npj Quantum Information* 8, 1 (Nov. 2022), 1–10. <https://doi.org/10.1038/s41534-022-00651-y>
- [21] Brett Giles and Peter Selinger. 2013. Exact synthesis of multiqubit Clifford+T circuits. *Phys. Rev. A* 87 (Mar 2013), 032332. Issue 3. <https://doi.org/10.1103/PhysRevA.87.032332>
- [22] David Gosset, Vadym Kliuchnikov, Michele Mosca, and Vincent Russo. 2013. An algorithm for the T-count. <https://doi.org/10.48550/arXiv.1308.4134> arXiv:1308.4134 [quant-ph].
- [23] Alexander S. Green, Peter LeFanu Lumsdaine, Neil J. Ross, Peter Selinger, and Benoît Valiron. 2013. Quipper: a scalable quantum programming language. *ACM SIGPLAN Notices* 48, 6 (June 2013), 333–342. <https://doi.org/10.1145/2499370.2462177>
- [24] Ali Javadi-Abhari, Matthew Treinish, Kevin Krsulich, Christopher J. Wood, Jake Lishman, Julien Gacon, Simon Martiel, Paul D. Nation, Lev S. Bishop, Andrew W. Cross, Blake R. Johnson, and Jay M. Gambetta. 2024. Quantum computing with Qiskit. arXiv:2405.08810 [quant-ph] <https://arxiv.org/abs/2405.08810>
- [25] Aleks Kissinger and John van de Wetering. 2020. PyZX: Large Scale Automated Diagrammatic Reasoning. *Electronic Proceedings in Theoretical Computer Science* 318 (May 2020), 229–241. <https://doi.org/10.4204/eptcs.318.14>
- [26] A. Yu. Kitaev. 1995. Quantum measurements and the Abelian Stabilizer Problem. arXiv:quant-ph/9511026 [quant-ph] <https://arxiv.org/abs/quant-ph/9511026>
- [27] A Yu Kitaev. 1997. Quantum computations: algorithms and error correction. *Russian Mathematical Surveys* 52, 6 (dec 1997), 1191. <https://doi.org/10.1070/RM1997v052n06ABEH002155>
- [28] Vadym Kliuchnikov, Dmitri Maslov, and Michele Mosca. 2012. Fast and efficient exact synthesis of single qubit unitaries generated by Clifford and T gates. <https://arxiv.org/abs/1206.5236v4>
- [29] E. Knill. 2004. Fault-Tolerant Postselected Quantum Computation: Schemes. arXiv:quant-ph/0402171 [quant-ph]
- [30] Andrew J. Landahl and Chris Cesare. 2013. Complex instruction set computing architecture for performing accurate quantum  $SZ$  rotations with less magic. <https://doi.org/10.48550/arXiv.1302.3240> arXiv:1302.3240 [quant-ph].
- [31] Gushu Li, Anbang Wu, Yunong Shi, Ali Javadi-Abhari, Yufei Ding, and Yuan Xie. 2022. Paulihedral: a generalized block-wise compiler optimization framework for Quantum simulation kernels. In *Proceedings of the 27th ACM International Conference on Architectural Support for Programming Languages and Operating Systems* (Lausanne, Switzerland) (ASPLOS '22). Association for Computing Machinery, New York, NY, USA, 554–569. <https://doi.org/10.1145/3503222.3507715>
- [32] Ben Mildenhall, Pratul P. Srinivasan, Matthew Tancik, Jonathan T. Barron, Ravi Ramamoorthi, and Ren Ng. 2020. NeRF: Representing Scenes as Neural Radiance Fields for View Synthesis. In *ECCV*.
- [33] Volodymyr Mnih, Koray Kavukcuoglu, David Silver, Alex Graves, Ioannis Antonoglou, Daan Wierstra, and Martin Riedmiller. 2013. Playing Atari with Deep Reinforcement Learning. arXiv:1312.5602 [cs.LG]
- [34] Lorenzo Moro, Matteo G. A. Paris, Marcello Restelli, and Enrico Prati. 2021. Quantum compiling by deep reinforcement learning. *Communications Physics* 4, 1 (Aug. 2021), 178. <https://doi.org/10.1038/s42005-021-00684-3>
- [35] Michael A. Nielsen and Isaac L. Chuang. 2011. *Quantum Computation and Quantum Information: 10th Anniversary Edition*. Cambridge University Press.
- [36] Joe O’Gorman and Earl T. Campbell. 2017. Quantum computation with realistic magic-state factories. *Physical Review A* 95, 3 (March 2017). <https://doi.org/10.1103/physreva.95.032338>
- [37] Anouk Paradis, Jasper Dekoninck, Benjamin Bichsel, and Martin Vechev. 2024. SynthetiQ: Fast and Versatile Quantum Circuit Synthesis.
- [38] Alberto Peruzzo, Jarrod McClean, Peter Shadbolt, Man-Hong Yung, Xiao-Qi Zhou, Peter J. Love, Alán Aspuru-Guzik, and Jeremy L. O’Brien. 2014. A variational eigenvalue solver on a photonic quantum processor. *Nature Communications* 5, 1 (July 2014). <https://doi.org/10.1038/ncomms5213>
- [39] Nils Quetschlich, Lukas Burgholzer, and Robert Wille. 2023. MQT Bench: Benchmarking Software and Design Automation Tools for Quantum Computing. *Quantum* (2023). <https://doi.org/10.22331/q-2023-07-20-1062> arXiv:2204.13719 [quant-ph] MQT Bench is available at <https://www.cda.cit.tum.de/mqtbench/>.
- [40] Nasim Rahaman, Aristide Baratin, Devansh Arpit, Felix Draxler, Min Lin, Fred A. Hamprecht, Yoshua Bengio, and Aaron Courville. 2019. On the Spectral Bias of Neural Networks. arXiv:1806.08734 [stat.ML]
- [41] Sebastian Rietsch, Abhishek Y. Dubey, Christian Ufrecht, Maniraman Periyasamy, Axel Plinge, Christopher Mutschler, and Daniel D. Scherer. 2024. Unitary Synthesis of Clifford+T Circuits with Reinforcement Learning. arXiv:2404.14865 [quant-ph]

- [42] F. Rosenblatt. 1958. The perceptron: A probabilistic model for information storage and organization in the brain. *Psychological Review* 65, 6 (1958), 386–408. <https://doi.org/10.1037/h0042519> Place: US Publisher: American Psychological Association.
- [43] Neil J. Ross and Peter Selinger. 2016. Optimal ancilla-free Clifford+T approximation of z-rotations. arXiv:1403.2975 [quant-ph]
- [44] Vivek V Shende, Stephen S Bullock, and Igor L Markov. 2006. Synthesis of quantum-logic circuits. *IEEE Transactions on Computer-Aided Design of Integrated Circuits and Systems* 25, 6 (2006), 1000–1010.
- [45] Peter W. Shor. 1995. Scheme for reducing decoherence in quantum computer memory. *Phys. Rev. A* 52 (Oct 1995), R2493–R2496. Issue 4. <https://doi.org/10.1103/PhysRevA.52.R2493>
- [46] Peter W. Shor. 1997. Polynomial-Time Algorithms for Prime Factorization and Discrete Logarithms on a Quantum Computer. *SIAM J. Comput.* 26, 5 (Oct. 1997), 1484–1509. <https://doi.org/10.1137/s0097539795293172>
- [47] Utkarsh Singhal, Yifei Xing, and Stella X. Yu. 2021. Co-domain Symmetry for Complex-Valued Deep Learning. arXiv:2112.01525 [cs.CV]
- [48] Seyon Sivarajah, Silas Dilkes, Alexander Cowtan, Will Simmons, Alec Edgington, and Ross Duncan. 2020. t|ket>: a retargetable compiler for NISQ devices. *Quantum Science and Technology* 6, 1 (Nov. 2020), 014003. <https://doi.org/10.1088/2058-9565/ab8e92>
- [49] Ethan Smith, Marc Grau Davis, Jeffrey Larson, Ed Younis, Lindsay Bassman Ofeltie, Wim Lavrijsen, and Costin Iancu. 2023. LEAP: Scaling Numerical Optimization Based Synthesis Using an Incremental Approach. *ACM Transactions on Quantum Computing* 4, 1, Article 5 (feb 2023), 23 pages. <https://doi.org/10.1145/3548693>
- [50] Richard S. Sutton and Andrew G. Barto. 2018. *Reinforcement Learning: An Introduction* (second ed.). The MIT Press.
- [51] Robert R. Tucci. 2005. An Introduction to Cartan’s KAK Decomposition for QC Programmers. arXiv:quant-ph/0507171 [quant-ph] <https://arxiv.org/abs/quant-ph/0507171>
- [52] Bo-Ying Wang and Fuzhen Zhang. 1994. A Trace Inequality for Unitary Matrices. *The American Mathematical Monthly* 101, 5 (1994), 453–455. <http://www.jstor.org/stable/2974909>
- [53] M. Weiden, E. Younis, J. Kalloor, J. Kubiawicz, and C. Iancu. 2023. Improving Quantum Circuit Synthesis with Machine Learning. In *2023 IEEE International Conference on Quantum Computing and Engineering (QCE)*. IEEE Computer Society, Los Alamitos, CA, USA, 1–11. <https://doi.org/10.1109/QCE57702.2023.00093>
- [54] Jonathan Welch, Daniel Greenbaum, Sarah Mostame, and Alán Aspuru-Guzik. 2014. Efficient Quantum Circuits for Diagonal Unitaries Without Ancillas. *New Journal of Physics* 16, 3 (March 2014), 033040. <https://doi.org/10.1088/1367-2630/16/3/033040> arXiv:1306.3991 [quant-ph].
- [55] Zhi-Qin John Xu. 2020. Frequency Principle: Fourier Analysis Sheds Light on Deep Neural Networks. *Communications in Computational Physics* 28, 5 (June 2020), 1746–1767. <https://doi.org/10.4208/cicp.oa-2020-0085>
- [56] Ed Younis and Costin Iancu. 2022. Quantum Circuit Optimization and Transpilation via Parameterized Circuit Instantiation. In *2022 IEEE International Conference on Quantum Computing and Engineering (QCE)*. 465–475. <https://doi.org/10.1109/QCE53715.2022.00068>
- [57] Yuan-Hang Zhang, Pei-Lin Zheng, Yi Zhang, and Dong-Ling Deng. 2020. Topological Quantum Compiling with Reinforcement Learning. *Physical Review Letters* 125, 17 (Oct. 2020). <https://doi.org/10.1103/physrevlett.125.170501>

## A Appendix

### A.1 Diagonal Distance

Our goal is to determine when a state  $s_t$  can be nearly inverted (satisfy the distance condition in Equation 6) by a completely diagonal unitary. Say the state of the synthesis process is  $s_t$ , and it is “nearly diagonal.” This means that each row of  $s_t$  is of the form

$$s_t[i] = \begin{bmatrix} \delta_{i1} & \dots & x_{ii} & \dots & \delta_{i2^n} \end{bmatrix}.$$

Because  $s_t$  is unitary, we know that  $|x_{ii}| = \sqrt{1 - \sum_{j \neq i} \delta_{ij}^2}$ . Consider a diagonal unitary matrix  $D$ , and the product  $D \times s_t$ . Rearranging the Hilbert-Schmidt distance function

$$\sqrt{4^n(1 - \epsilon^2)} \leq |\text{tr}(D \times s_t)| \leq \sum_i |d_{ii}| \cdot |x_{ii}| \leq \sum_i |x_{ii}|$$

then it is the case that

$$2^n \sqrt{(1 - \epsilon^2)} \leq \sum_{i=1}^{2^n} \sqrt{1 - \sum_{j \neq i} \delta_{ij}^2} \leq \max_{i \in [2^n]} 2^n \sqrt{1 - \sum_{j \neq i} \delta_{ij}^2}$$

which can be reduced to

$$\max_{i \in [2^n]} \sqrt{\sum_{j \neq i} \delta_{ij}^2} \leq \epsilon.$$

Thus, if the maximum magnitude of non-diagonal row elements is less than the synthesis threshold, state  $s_l$  can be multiplied by a purely diagonal matrix so that the Hilbert-Schmidt distance condition is met.

## A.2 Global Phase Invariance

For unitary  $U$ , we define  $\mu = \frac{1}{N^2} \sum u_{ij} \in \mathbb{C}$  to be the element-wise mean. As it may be the case that  $\mu = 0$ , we consider the mean of the element-wise squared matrix  $U^{\odot 2}$  which is  $\mu' = \frac{1}{N^2} \sum u_{ij}^2$ . We normalize this to obtain  $\hat{\mu}' = \mu' / \|\mu'\|$ . Next we halve the phase of  $\hat{\mu}'$  and conjugate to receive  $\hat{\mu}^*$ . Finally we multiply by  $U$  and conditionally add a phase correction of  $\pi$  to receive a global phase invariant representation  $W$ . This process is depicted in Figure 5.

**PROOF.** Say  $U = e^{i\theta}W$ . The element-wise mean of  $U^{\odot 2}$  is  $\mu' = e^{i(2\theta+2\pi k)}x$ . Normalizing, halving the phase, and conjugating gives  $\hat{\mu}^* = e^{-i(\theta+k\pi)}$ . Multiplying  $U$  by the conjugated normalized mean gives  $\hat{\mu}^*U = e^{i\theta}e^{-i(\theta+k\pi)}W = e^{-ik\pi}W$ . From this final result we cannot detect whether  $k$  is odd or even. We choose to ensure that the first maximum magnitude entry of the first row of  $W$  should have a positive real component. If it does not, we apply the  $\pi$  phase correction.  $\square$

Received 15 October 2024